Process Linearization for Closed-Loop Control of Incremental Sheet Forming

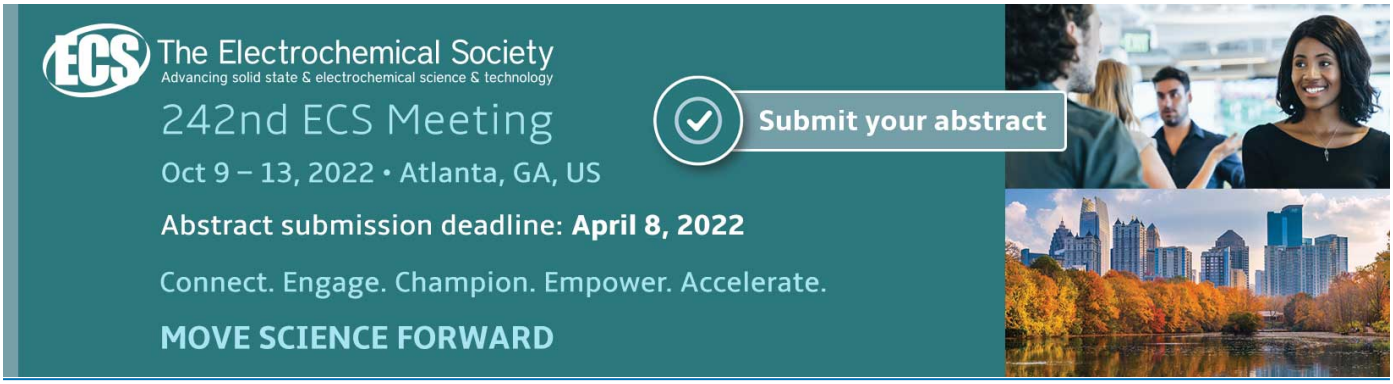

Process Linearization for Closed-Loop Control of Incremental Sheet Forming

Jos Havinga, Dylan Sikkelbein and Ton van den Boogaard
University of Twente, Enschede, The Netherlands
E-mail: jos.havinga@utwente.nl

Abstract. Incremental sheet forming has, despite its great flexibility, not yet been widely adopted by the forming industry, due to its limited geometric accuracy. One of the approaches to overcome this problem is the development of closed-loop control systems. Such control systems are mostly based on linearization with respect to a nominal toolpath. In this work, different approaches to create such linearized process models are reviewed. By implementing the models in a numerical simulation of a model predictive control system for incremental sheet forming, it is investigated how manufacturing accuracy is affected by the chosen linearization. Based on these results, the validity of the most commonly used linearization method is critically discussed. Furthermore, it is shown that the geometric accuracy can be improved by extending the process model with a time-varying component that contains historical information about past control actions.

1. Introduction

The history of Incremental Sheet Forming (ISF) dates back to the publication of several patents in the 60's [1]. From the 90's onwards, the attention of the metal forming research community for these types of processes has gradually increased [2, 3]. The major advantages of ISF over conventional sheet forming processes (e.g. deepdrawing) are enhanced formability [4] and high flexibility of the manufacturing process, as ISF does not require product-specific tools. Although these advantages have attracted many researchers to ISF, these processes have not yet been widely adopted in industry, due to relatively long production times and low geometrical accuracy, which is caused by springback.

In a review paper from 2005, Jeswiet et al. predicted that the disadvantage of lower geometrical accuracy would be dealt with by the development of new algorithms [2]. Indeed, a large number of publications have been devoted to the improvement of the geometrical accuracy of ISF [5]. Different methods have been studied to achieve this, such as local heating of the sheet [6, 7], multi-stage forming [8], flexible support of the sheet (e.g. two-point incremental forming) [9], toolpath optimization [10, 11] or closed-loop control [12].

Several of the proposed toolpath optimization methods can be considered to be a type of part-to-part control or iterative learning control method, because they use geometry measurements from a (series of) product(s) to adjust the toolpath for a next product. In the present work, we focus on closed-loop control of ISF, meaning that control systems are considered where measurements during forming of a single product are used to adjust the process conditions (i.e. toolpath) for that same product. The basis for these type of ISF control systems was laid in the work of Allwood et al. by presenting the concept of linearization around a pre-planned toolpath

[12]. The idea is to define a nominal toolpath and create a linear model that relates deviations from the nominal toolpath to changes of product geometry. Such a model can be used to predict the final geometry of a product during forming. The model can therefore be used in a control system. This approach has been applied to ISF by several researchers, mostly in combination with a Model Predictive Control (MPC) system [13–17].

Linearization of highly nonlinear forming processes can be justified by the requirement that the deviations with respect to the nominal toolpath must be small. Furthermore, limited model errors are acceptable as the closed-loop corrections can compensate for these errors. This is supported by several numerical and experimental results for products with limited complexity [12–17]. It can however be expected that the quality of the linearized process model will have a major effect on the performance of these control systems. Different methods for toolpath linearization for ISF will therefore be investigated in this work, and the effect of these methods on the performance of the control system will be analysed in a numerical study. Better understanding about such models may be used to improve the performance of existing MPC systems for ISF, as well as to enlarge the applicability of such systems to more complex products.

The methods for toolpath linearization will be discussed in Section 2. The MPC system will be explained in Section 3. The relation between linearization method and MPC performance will be studied using simulation models for products with varying complexity. These simulation models will be presented in Section 4. The linearized process models as well as the MPC performance will finally be presented in Section 5, followed by a discussion in Section 6.

2. Process Linearization for Incremental Sheet Forming

The concept of toolpath linearization for ISF was proposed in the work of Allwood et al. [12]. Given a discretization of the toolpath into K steps, they propose that the state of the product $\mathbf{z}_k$ (after step k) can be approximated as the previous state plus the product between a vector $\mathbf{g}_k$ and a scalar u_k that represents the size of a control action for step k:

$$\mathbf{z}_k \approx \mathbf{z}_{k-1} + \mathbf{g}_k u_k \tag{1}$$

This can be extended to the relation between the final state $\mathbf{z}_K$, the intermediate state $\mathbf{z}_k$, and all control actions that are executed after step k, $\{u_i \,|\, i = k+1, \ldots, K\}$:

$$\mathbf{z}_K \approx \mathbf{z}_k + \sum_{i=k+1}^{K} \mathbf{g}_i u_i \tag{2}$$

In the linearization it is assumed that each control action u_i causes a change of size $\mathbf{g}_i u_i$ to the state of the product. Local deformation, plastic strain and residual stress can all be considered to be part of the state $\mathbf{z}_k$. For simplicity of the approach, only the deformation of the product is included in the state vector $\mathbf{z}_k$. In that case, $\mathbf{g}_i u_i$ is the change of shape of the product caused by step i, which is thus assumed to be proportional to the size of the control action u_i. The toolpath can be discretized in many different ways, but in this work it is chosen to discretize the toolpath as a series of z-level contours (Figure 1): the tool follows a specified contour in x-y plane at different depths (the z-levels). In the linearization given above, u_k represents the distance between two subsequent z-levels.

The derivation of Eq.(2) is given in the work of Allwood et al. [12]. It effectively states that each term $\mathbf{g}_i u_i$ represents the change of shape between two subsequent contours. The vector $\mathbf{g}_i$ is considered to be an impulse response, as discussed in detail in the work of Music et al. [18]. This approach is also taken in several of the works that build upon this proposal. In this work we refer to this linearization as *Def. 1 - Full step* .

In the derivation, the concept of toolpath linearization is used, and by taking a different route a slightly different form of the linearizaiton can be derived as well. Assume a nominal toolpath

$\{\bar{u}_k \,|\, k = 1, \ldots, K\}$ to be the series of z-level increments that correspond to a pre-planned path. The state evolution for the nominal process will then be $\{\bar{\mathbf{z}}_k \,|\, k = 1, \ldots, K\}$. A correction Δu_k with respect to the nominal tool path can be defined as $\Delta u_k = u_k - \bar{u}_k$, where u_k is the actual step size between to subsequent contours, as shown in Figure 1. Linearizing the process with respect to the correction Δu_k gives the following relation between two subsequent states:

$$\mathbf{z}_k \approx \mathbf{z}_{k-1} + \bar{\mathbf{z}}_k - \bar{\mathbf{z}}_{k-1} + \mathbf{g}_k \Delta u_k \tag{3}$$

The terms $\bar{\mathbf{z}}_k - \bar{\mathbf{z}}_{k-1}$ represent the change of state in the nominal process between two subsequent steps, and the term $\mathbf{g}_k \Delta u_k$ represents the effect of a correction with respect to the planned nominal step size $\bar{u}_k$. The equation above can be extended to the relation between intermediate state $\mathbf{z}_k$ and final state $\mathbf{z}_K$ as:

$$\mathbf{z}_K \approx \mathbf{z}_k + \bar{\mathbf{z}}_K - \bar{\mathbf{z}}_k + \sum_{i=k+1}^{K} \mathbf{g}_i \Delta u_i \tag{4}$$

In this work, this definition is referred to as *Def. 2 - Correction* . Note that, if the linearity assumption from Eq.(1) holds, Eq.(3) will be merely a rewritten form of Eq.(1), because it will then also hold that $\bar{\mathbf{z}}_k - \bar{\mathbf{z}}_{k-1} = \mathbf{g}_k \Delta u_k$. However, if the nonlinearity is significant, it may be better to perform a linearization that remains close to the nominal toolpath, as in Eq.(3).

The impulse responses $\{\mathbf{g}_k \,|\, k = 1, \ldots, K\}$ can be determined experimentally or numerically. Such a procedure can be sensitive to noise, and therefore some researchers have simplified the impulse responses by fitting it to predefined mathematical functions, such as the cumulative Weibull distribution [12, 13]. This approach is also investigated in this work, and the impulse responses that are fitted with the Weibull function are referred to as *Def. 3 - Weibull fit* .

The final linearization method that will be considered in this work is based on the observation that Eq.(4) implies that the effect of a control action is instantaneous (the effect of Δu_k can be seen at state $\mathbf{z}_k$) and that the effect remains constant during all future steps. This can be understood as follows: consider that the correction Δu_k is applied at step k, and that all future corrections $\{\Delta u_i \,|\, i = k+1, \ldots, K\}$ are set to zero. According to Eq.(3), the change in state between step $k-1$ and step m (with $m \geq k$) will be equal to $\bar{\mathbf{z}}_m - \bar{\mathbf{z}}_{k-1} + \mathbf{g}_k \Delta u_k$. However, the properties (residual stress, plastic strain, etc.) of the product have changed due to the correction Δu_k, and therefore it could be that the product will respond differently to the upcoming sequence of nominal steps $\{\bar{u}_i \,|\, i = k+1, \ldots, K\}$. In other words, the change of state between steps $k-1$ and k may be affected by all past corrections $\{\Delta u_i \,|\, i = 1, \ldots, k\}$ as well:

$$\mathbf{z}_k \approx \mathbf{z}_{k-1} + \bar{\mathbf{z}}_k - \bar{\mathbf{z}}_{k-1} + \sum_{i=1}^{k} \mathbf{g}_{i,k} \Delta u_i \tag{5}$$

In this equation, $\mathbf{g}_{i,k} \Delta u_i$ represents the change of state from step $k-1$ to step k, caused by the previously applied correction Δu_i (with $i \leq k$). When accounting for this effect, the relation between intermediate state $\mathbf{z}_k$ and final state $\mathbf{z}_K$ can be written as:

$$\mathbf{z}_K \approx \mathbf{z}_k + \bar{\mathbf{z}}_K - \bar{\mathbf{z}}_k + \sum_{j=k+1}^{K} \sum_{i=1}^{k} \mathbf{g}_{i,j} \Delta u_i + \sum_{i=k+1}^{K} \mathbf{g}_i \Delta u_i \tag{6}$$

The term with the vectors $\mathbf{g}_{i,j}$ represents the changes of the state caused by all past corrections $\{\Delta u_i \,|\, i = 1, \ldots, k\}$, and the term with the impulse responses $\mathbf{g}_i$ represents the changes of the state to be caused by all future corrections $\{\Delta u_i \,|\, i = k+1, \ldots, K\}$. In this work, this linearization approach is referred to as as *Def. 4 - History aware* .

The different linearized models are given by Eqs.(2), (4) and (6). The impulse responses for all different linearizations can be determined by experiments or simulations [12, 18]. From practical point of view, it is relevant how much effort is required to obtain all impulse responses. In that perspective, it is clear that *Def. 1 - Full step* can be determined with significantly less experiments or simulations. It is however out of the scope of this work to account for the complexity and cost of determining the linearized process model. In this work, it will be investigated whether it is helpful to use a more extensive linearized process model. In future work, it may be investigated how such a detailed process model can be approximated with limited effort. In Section 5.1, the differences between the impulse responses will be presented for an axisymmetric cone.

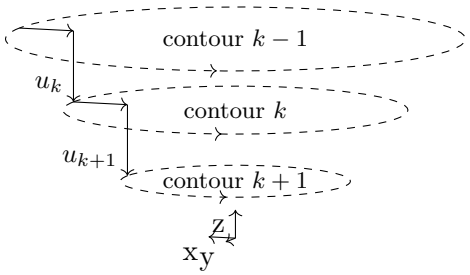

Figure 1. Z-level contours.

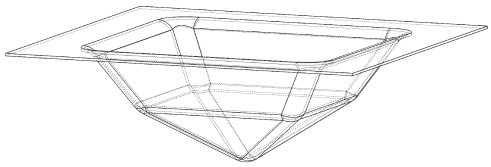

Figure 2. Shape of two-angle pyramid target product.

3. Model Predictive Control

Given a target final state $\hat{\mathbf{z}}_K$, and a final state $\tilde{\mathbf{z}}_K$ as predicted by the process model $f(\mathbf{z}_k, \Delta\mathbf{u}_k)$, the optimal control actions can be determined using the following Model Predictive Control optimization problem:

$$\begin{aligned} \underset{\Delta\mathbf{u}_k}{\text{minimize}} \quad & \|\tilde{\mathbf{z}}_K - \hat{\mathbf{z}}_K\|_2 + \alpha\|\Delta\mathbf{u}_k\|_2 \\ \text{subject to} \quad & \tilde{\mathbf{z}}_K = f(\mathbf{z}_k, \Delta\mathbf{u}_k), \\ & lb \leq \Delta u_i \leq ub \quad \forall\ i \end{aligned} \tag{7}$$

Where $\Delta\mathbf{u}_k = [\Delta u_{k+1}, \ldots, \Delta u_K]^T$ is a vector with all future control actions, and lb and ub are the lower bound and upper bound for the control actions respectively. The intermediate state $\mathbf{z}_k$ is obtained by measurement. The MPC problem can be solved efficiently with any of the linearized models (Eqs.(2), (4) or (6)) using quadratic programming. After each step, the state of the product is measured again, and a new optimal control sequence can be determined, of which the first control action Δu_{k+1} is applied to the process. The α parameter can be used to limit the magnitude of the control actions.

4. Single Point Incremental Forming Simulation Model

A series of simulations have been conducted to evaluate the effect of the linearization assumption on the performance of MPC for ISF. As modelling implies simplification by definition, and the aim of this numerical study is conceptual understanding, it is not attempted to validate all underlying physics, such as friction and material models. The results of this study are indicative, but require additional investigation to be validated with a specific test case.

A Single Point Incremental Forming (SPIF) simulation model was created using the finite element package Abaqus. A square sheet with edges of 150 mm and thickness of 1 mm was meshed with approximately 4500 linear quadrilateral reduced integration shell elements. All degrees of freedom at the edges have been constrained. The hardening function $\sigma_y = 390\varepsilon_p^{0.19}$ is

used to represent the aluminium alloy AlMg3. A spherical tool with diameter of 15 mm follows a series of z-level contours. The nominal step size $\bar{u}_k$ is -1 mm. Three different shapes have been investigated. A straight cone and a two-angle cone are both axi-symmetric, and shown in Figure 3. The nominal toolpath is determined using the target geometry and tool radius only, by assuming that the tool is just touching the target shape at each z-level contour. Due to springback, the final shape of the product will be less deep, as visualized in Figure 3. At the inside (radius $\leq$ 10 mm) and the outside (radius $\geq$ 40 mm) of the product, the actual shape of the product deviates from the target shape in a way that cannot be corrected with any toolpath. Therefore, a region of interest is defined, in which the MPC is used to minimize the error between actual shape and target shape.

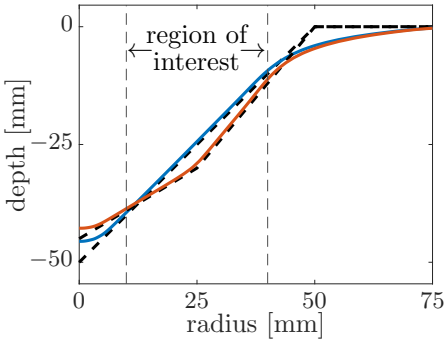

Figure 3. Target shapes $\hat{\mathbf{z}}_K$ (- -) and nominal final shape $\mathbf{z}_K$ of straight cone (—) and two-angle cone (—).

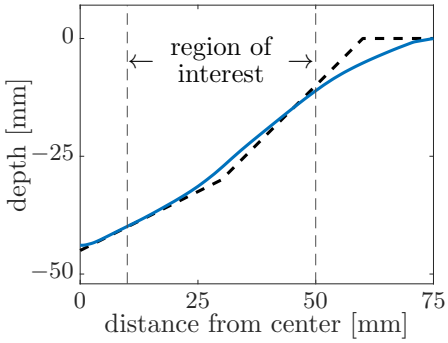

Figure 4. Target shape $\hat{\mathbf{z}}_K$ (- -) and nominal final shape $\mathbf{z}_K$ of two-angle pyramid at the center of the sides (—).

These two target products are relatively simple to control due to their axi-symmetry. In contrast, a two-angle pyramid (Figure 2) poses additional challenges to the controller due to the 'tent effect' [11]. The product is formed from the outside to the inside, and after the tool passes the change in wall angle (at 30 mm from the center), the upper part of the product is pulled inwards, causing a significant deviation from the target shape in the region of the change in wall angle. To simplify the analysis, only the centers of the sides of the pyramid are considered, and the shape at the corners of the two-angle pyramid is not accounted for. The target shape and the final shape from the simulation with nominal toolpath are shown in Figure 4.

Another simplification is that the tool is retracted after each z-level contour. A measurement is taken without tool contact, and the effect of springback is therefore removed from the problem. The MPC control sequence is simulated by connecting the Abaqus model with MATLAB, that is used to evaluate the simulation results from each step, calculate the new control action, and restart the simulation with an adjusted toolpath.

5. Results

Many simulation runs with the above-mentioned model have been performed, first to determine all impulse responses, and then to perform MPC simulations. The characteristics of the impulse responses are presented in Section 5.1, and the results for the axi-symmetric products and the square pyramid are presented in Sections 5.2 and 5.3 respectively.

5.1. Impulse responses

The impulse responses for *Def. 1 - Full step* have been determined using a single simulation with the nominal toolpath. The impulse responses for the other linearizations have been determined using K simulations, in which a correction Δu_k was applied at one of the steps, with all other

corrections set to zero. The effect of all control actions on all future states could be determined by comparing the shape after each step with the shape at the same step in the nominal simulation. The size of the applied corrections Δu_k was set to $\pm$ 0.6 mm. The results with both positive (less deep) and negative (deeper) corrections are shown in Figure 5. It is expected that both positive and negative corrections must be applied during control. The data shows that there is no linear relation between control action and impulse response throughout the full control action space, which raises the question which linearization is best to use.

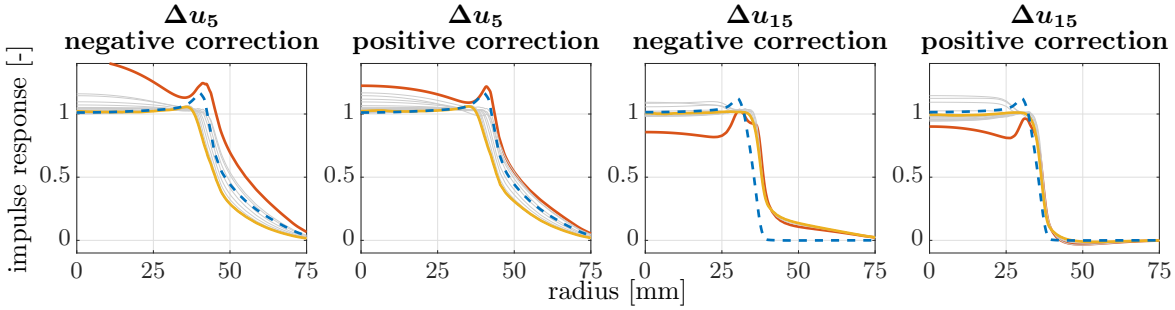

Figure 5. Impulse responses determined with negative (-0.6 mm) and positive (0.6 mm) corrections to the toolpath. The effect at step k (—) and at the final step K (—) are shown, as well as the effect on all intermediate steps (in grey). The impulse response determined with *Def. 1 - Full step* is also shown (- -).

It is also clear from Figure 5 that the effect of correction Δu_k is not constant over all future steps, as assumed in *Def. 1 - Full step* , *Def. 2 - Correction* and *Def. 3 - Weibull fit* . It is therefore required to use *Def. 4 - History aware* to account for this effect. For *Def. 2 - Correction* and *Def. 3 - Weibull fit* , the effect of a correction on the shape at the final step K (— lines in Figure 5) is used in the process models.

5.2. Axisymmetric cones

The deviation between the final geometry and the target shape is shown in Figure 6 for different MPC runs of the straight cone. As a reference, the nominal toolpath results in a geometry with a Root Mean Squared Error (RMSE) of 0.653 mm. The MPC system dramatically reduces the error, although it is important to note that the current simulation setting is not a valid reference for a real experiment, as the process models are determined with the same simulations that is used for the MPC runs. When comparing the different approaches, it can be seen that *Def. 1 - Full step* yields the highest RMSE (0.040 mm), and that *Def. 4 - History aware* gives the lowest RMSE (0.020 mm). Furthermore, the differences between the solid and dashed lines indicate that whether a process model has been defined with positive of negative correction has a significant effect on the results.

The linearization of the straight cone has been reused in a model for forming a two-angle cone, in order to test the range of validity of the linearized model. The only difference in the used equations is that the nominal state evolution $\bar{\mathbf{z}}_i$ has been updated using this linearization. Again, the MPC control results in Figure 8 show much lower RMSE than observed in the nominal run (0.645 mm). For all methods, the linearization that is defined with a positive correction performs best. Again, the highest and lowest RMSE are obtained with *Def. 1 - Full step* (0.075 mm) and *Def. 4 - History aware* (0.050 mm) respectively.

5.3. Two-angle pyramid

The two-angle pyramid shape is the most challenging product that is investigated due to the tent-effect. In case of an uncontrolled run with the nominal toolpath, the RMSE is 1.25 mm.

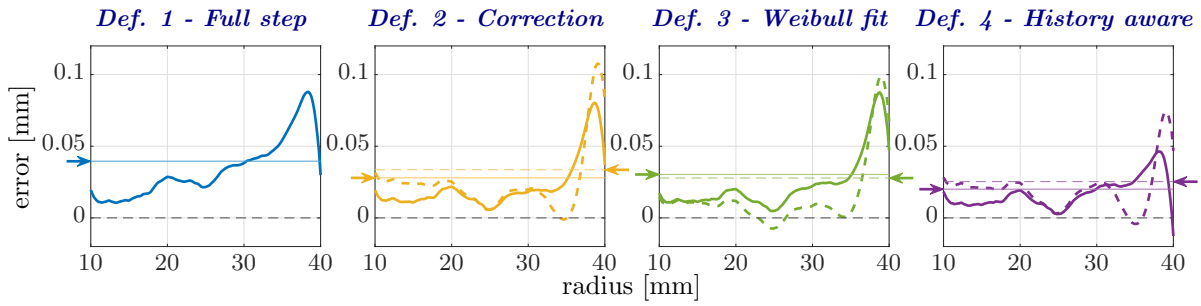

Figure 6. Deviation to target shape for all straight cone MPC runs. When applicable, a dashed and a solid line are used for the results of process models that have been determined with a negative correction and a positive correction respectively. The horizontal line that is highlighted with an arrow indicates the RMSE over the complete region of interest.

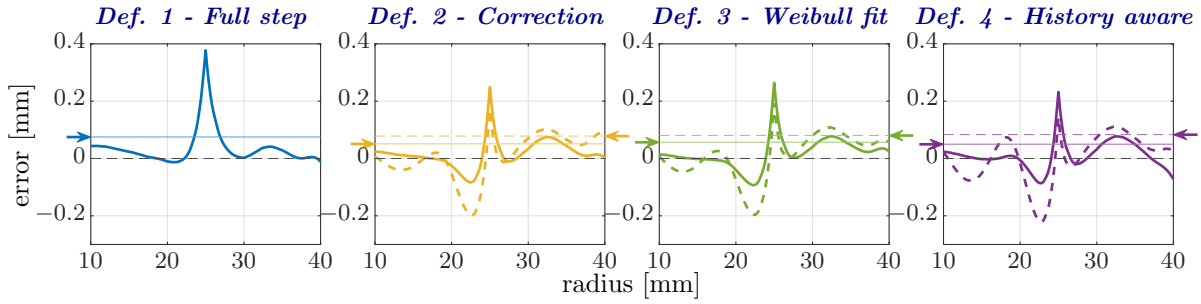

Figure 7. Deviation to target shape for all two-angle cone MPC runs. The meaning of different line styles is explained in the caption of Figure 6.

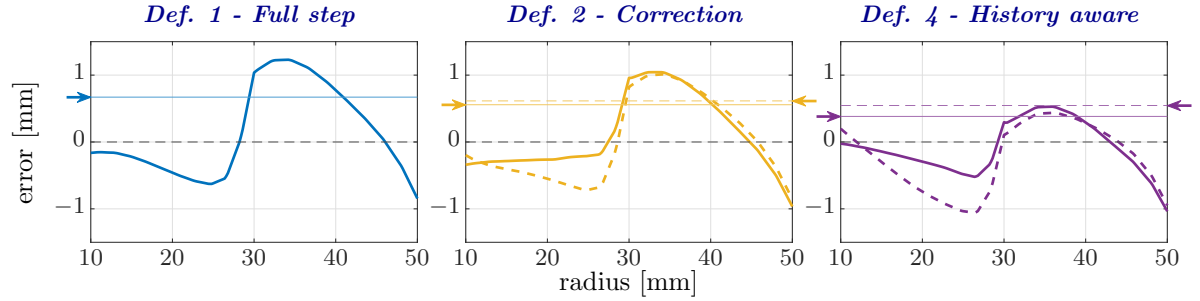

Figure 8. Deviation to target shape for all two-angle pyramid MPC runs. The meaning of different line styles is explained in the caption of Figure 6.

This can be reduced to 0.67 mm using *Def. 1 - Full step* , 0.56 mm using *Def. 2 - Correction* and 0.38 mm using *Def. 4 - History aware* . Again, the best solutions are obtained using the most elaborated linearization. Also, the same trend as for the other products is seen: the linearizations that have been determined with a positive correction perform best.

6. Discussion

A numerical investigation about the effect of linearization methods on MPC performance for ISF is presented in this work. It was shown how different assumptions can be used to obtain different linearizations with respect to a pre-planned toolpath. As the detail and accuracy of these linearizations differ, it is expected that the linerization model affects the MPC performance. It was shown for three different products that the best MPC results can be obtained with the

most extended linearization, that accounts for the nominal evolution of the state as well as for the observation that the effect of a control action is not constant with respect to all future states. In comparison with *Def. 1 - Full step* , which is mostly used in literature, the extensive linearization of *Def. 4 - History aware* was able to reduce the RSME from 0.040 mm to 0.020 mm for the straight cone, from 0.075 mm to 0.050 mm for the two-angle cone, and from 0.067 mm to 0.038 mm for the two-angle pyramid.

These results must be assessed in the practical context of ISF control. This work shows that better linearization methods can be used to improve MPC performance for ISF. To continue the development of closed-loop control systems for ISF, it must be answered what type of models and control algorithms are needed to achieve certain levels of production accuracy, and how part complexity imposes specific requirements for models and algorithms. Potentially, additional state variables may be required to improve process model accuracy and to include additional constraints, such as for thinning. Such state variables may have to be estimated using dedicated measurement models and indirect measurements such as process forces. Furthermore, it will be the question how to obtain the required process models with limited experimental and numerical cost, and how to include knowledge about modelling uncertainty into the control system. By addressing these questions, the applicability of closed-loop control for complex ISF products may become closer, significantly improving the potential of ISF for the industrial practice.

References

[1] Emmens W C, Sebastiani G and van den Boogaard A H 2010 *Journal of Materials Processing Technology* **210** 981–997
[2] Jeswiet J, Micari F, Hirt G, Bramley A, Duflou J and Allwood J 2005 *CIRP Annals* **54** 88–114
[3] Duflou J R, Habraken A M, Cao J, Malhotra R, Bambach M, Adams D, Vanhove H, Mohammadi A and Jeswiet J 2017 *International Journal of Material Forming* **11** 743–773
[4] Emmens W C and van den Boogaard A H 2009 *Journal of Materials Processing Technology* **209** 3688–3695
[5] Micari F, Ambrogio G and Filice L 2007 *Journal of Materials Processing Technology* **191** 390–395
[6] Duflou J R, Callebaut B, Verbert J and De Baerdemaeker H 2007 *CIRP Annals* **56** 273–276
[7] Fan G, Gao L, Hussain G and Wu Z 2008 *International Journal of Machine Tools and Manufacture* **48** 1688–1692
[8] Bambach M, Taleb Araghi B and Hirt G 2009 *Production Engineering* **3** 145–156
[9] Reddy N V, Lingam R and Cao J 2015 *Incremental Metal Forming Processes in Manufacturing* (London: Springer London) pp 411–452 ISBN 978-1-4471-4670-4
[10] Hirt G, Ames J, Bambach M, Kopp R and Kopp R 2004 *CIRP Annals* **53** 203–206
[11] Behera A K, Verbert J, Lauwers B and Duflou J R 2013 *Computer-Aided Design* **45** 575–590
[12] Allwood J M, Music O, Raithathna A and Duncan S R 2009 *CIRP Annals* **58** 287–290
[13] Wang H and Duncan S 2010 *IET Conference Proceedings* 1172–1177(5)
[14] Lu H, Kearney M, Li Y, Liu S, Daniel W J T and Meehan P A 2015 *The International Journal of Advanced Manufacturing Technology* **82** 1781–1794
[15] Lu H, Kearney M, Wang C, Liu S and Meehan P A 2017 *Precision Engineering* **49** 179–188
[16] He A, Kearney M P, Weegink K J, Wang C, Liu S and Meehan P A 2020 *The International Journal of Advanced Manufacturing Technology* **107** 123–143
[17] He A, Wang C, Liu S and Meehan P A 2020 *Journal of Manufacturing Processes* **53** 342–355
[18] Music O and Allwood J M 2012 *Journal of Materials Processing Technology* **212** 1139–1156